

Numerical Renormalization Group Approach to a Quantum Dot Coupled to Normal and Superconducting Leads

Yoichi Tanaka¹, Norio Kawakami^{1,2}, and Akira Oguri³

¹*Department of Applied Physics, Osaka University, Suita, Osaka 565-0871, Japan*

²*Department of Physics, Kyoto University, Kyoto 606-8502, Japan*

³*Department of Material Science, Osaka City University, Osaka 558-8585, Japan*

We study transport through a quantum dot coupled to normal and superconducting leads using the numerical renormalization group method. We show that the low-energy properties of the system are described by the local Fermi liquid theory despite of the superconducting correlations penetrated into the dot due to a proximity effect. We calculate the linear conductance due to the Andreev reflection in the presence of the Coulomb interaction. It is demonstrated that the maximum structure appearing in the conductance clearly characterizes a crossover between two distinct spin-singlet ground states, i.e. the superconducting singlet state and the Kondo singlet state. It is further elucidated that the gate-voltage dependence of the conductance shows different behavior in the superconducting singlet region from that in the Kondo singlet region.

KEYWORDS: quantum dot, Andreev reflection, Kondo effect, numerical renormalization group method

1. Introduction

Recent progress in nano-technology has attracted much interest in studying quantum transport in mesoscopic systems. Among others, a quantum dot (QD)¹ has played an important role to reveal correlation effects in the nanoscale systems. In particular, the observation^{2,3} of the Kondo effect in QD systems⁴⁻⁸ opened a systematic way to investigate strongly correlated electrons, which has encouraged further theoretical and experimental studies in this field. Besides this substantial progress, transport properties of a mesoscopic system with hybrid normal(metal)-superconductor junctions have been also investigated extensively. In this system, the Andreev reflection⁹ plays a key role in physics, in which an incoming electron from normal side can be reflected as a hole, therefore transferring a Cooper pair into superconductor.

The above interesting topics in nanoscale systems naturally stimulated the research on the Andreev reflection for a QD coupled to normal and superconducting leads (N-QD-S).¹⁰⁻¹⁵ In this system, the Andreev reflection (the proximity effect) at the QD-S interface induces the superconducting correlation in the QD, which has a tendency to form the spin-singlet state. On the other hand, for large Coulomb interactions, the Kondo effect is enhanced and therefore the Kondo spin-singlet state is stabilized between the spin moment in the QD and the conduction electrons in the leads. Thus, the competition between these two distinct spin-singlet states occurs in the N-QD-S system. In order to clarify how this competition affects the transport in this system, theoretical analyses¹⁶⁻²⁷ as well as experimental investigations²⁸ have been done intensively, *e.g.* the linear^{16, 17, 19, 21, 25, 28} or nonlinear^{16, 18, 22, 23, 25, 27, 28} conductance, the excess Kondo resonance coming from the novel co-tunneling process (Andreev-normal co-tunneling),²⁰ the Andreev reflection through a QD embedded in an Aharonov-Bohm ring²⁴ and the adiabatic electron pumping²⁶ etc.

In particular, some theoretical studies on the linear conductance have clarified that the Coulomb interaction suppresses the Andreev reflection at the QD-S interface, which leads to the decrease of the linear conductance.^{16, 17, 19, 25} However, these studies have been done on the assumption that the Coulomb interaction in the QD is sufficiently large. On the other hand, Cuevas *et al.* analyzed the conductance over the range from the non-interacting case to the strong-correlation limit, using a modified second-order perturbation theory.²¹ They found that the increase of the coupling between the QD and the superconducting lead makes it possible to restore the conductance possibly up to the maximum value $4e^2/h$, although physical implications of the conductance maximum in the presence of the Coulomb interaction were not discussed in detail. In an N-QD-S system, moreover, the total number of electrons is not conserved, because of the superconducting correlation. In such a system, it is not obvious whether the low-energy properties are described by the local Fermi liquid theory.

In this paper, we theoretically investigate the transport in an N-QD-S system with the use of the numerical renormalization group (NRG) method,^{29,30} which has been applied successfully to a Josephson current through a QD.³¹⁻³³ Applying the Bogoliubov transformation, we first show that the low-energy properties of an N-QD-S system are described by the local Fermi liquid theory. Using the NRG method, we calculate the conductance due to the Andreev reflection with high accuracy and thus confirm Cuevas *et al.*'s results. To understand the behavior of the conductance, the renormalized parameters, which characterize the Andreev bound states around the Fermi energy, are calculated. From the analysis of the ground state properties, we demonstrate that the conductance maximum clearly characterizes a crossover between the superconducting singlet state and the Kondo singlet state.

This paper is organized as follows. In the next section, we introduce the model and describe the low-energy properties in terms of the local Fermi liquid theory. Then in §3, we calculate the conductance and the renormalized parameters. We discuss how the interplay between the Kondo effect and the superconducting correlation is reflected in the transport, by systematically changing the Coulomb interaction, the tunneling amplitude and the gate voltage. A brief summary is given in the last section.

2. Model and Formulation

2.1 Model

The Hamiltonian of a QD coupled to normal (N) and superconducting (S) leads is given by

$$H = H_d^0 + H_d^U + H_S + H_N + H_{TS} + H_{TN}, \quad (1)$$

where $H_d^0 + H_d^U$ and $H_{S(N)}$ represent the QD part and the superconducting (normal) lead part, respectively. H_{TS} and H_{TN} are the mixing terms between the QD and the leads. The explicit form of each part reads

$$H_d^0 = \left(\varepsilon_d + \frac{U}{2} \right) (n_d - 1), \quad H_d^U = \frac{U}{2} (n_d - 1)^2,$$

$$H_S = \sum_{q,\sigma} \varepsilon_q s_{q\sigma}^\dagger s_{q\sigma} + \sum_q (\Delta s_{q\uparrow}^\dagger s_{-q\downarrow}^\dagger + \text{H.c.}),$$

$$H_N = \sum_{k,\sigma} \varepsilon_k c_{k\sigma}^\dagger c_{k\sigma}, \quad H_{TN} = \sum_{k,\sigma} \frac{V_N}{\sqrt{M_N}} (c_{k\sigma}^\dagger d_\sigma + \text{H.c.}),$$

$$H_{TS} = \sum_{q,\sigma} \frac{V_S}{\sqrt{M_S}} (s_{q\sigma}^\dagger d_\sigma + \text{H.c.}). \quad (2)$$

The operator d_σ^\dagger creates an electron with energy ε_d and spin σ at the QD, and $n_d = \sum_\sigma d_\sigma^\dagger d_\sigma$. Following ref. 29, we here write down the QD part $H_d^0 + H_d^U$ in such a way that the energy of the one-electron occupied state ($n_d = 1$) is zero. Note that $H_d^0 + H_d^U = \varepsilon_d n_d + U n_{d\uparrow} n_{d\downarrow} + \text{const.}$, because $(n_d - 1)^2 = 2n_{d\uparrow} n_{d\downarrow} - n_d + 1$. In this representation, H_d^0 gives the energy shift due to the deviation from the electron-hole symmetric case ($\varepsilon_d + U/2 = 0$). In the Hamiltonian for leads, $s_{q\sigma}^\dagger (c_{k\sigma}^\dagger)$ is the creation operator of an electron with the energy $\varepsilon_q (\varepsilon_k)$ in the superconducting (normal) lead. In $H_{TS} (H_{TN})$, $V_S (V_N)$ is the tunneling amplitude between the QD and the superconducting (normal) lead, and $M_S (M_N)$ is the number of lattice sites in the superconducting (normal) lead. We assume that the superconducting lead is well described by the BCS theory with a superconducting gap $\Delta = |\Delta| e^{i\phi_S}$, where ϕ_S is the phase of the superconducting gap.

In what follows, we consider the limiting case of $|\Delta| \rightarrow \infty$. The essential physics of the Andreev reflection, which occurs inside the superconducting gap, is still captured in this limit. In this situation, the Hamiltonian (1) can be reduced exactly to an effective single-channel Hamiltonian (see Appendix A)^{32,34}

$$H^{\text{eff}} = H_d^0 + H_d^U + H_d^{\text{SC}} + H_N + H_{TN}, \quad (3)$$

where

$$H_d^{\text{SC}} = \Delta_d d_\uparrow^\dagger d_\downarrow^\dagger + \text{H.c.} \quad (4)$$

H_d^{SC} denotes the effective onsite superconducting gap at the QD,

$$\Delta_d \equiv \Gamma_S e^{i\phi_S}. \quad (5)$$

Notice here that the resonance strength between the QD and the superconducting lead is given by $\Gamma_S(\varepsilon) = \pi \sum_q V_S^2 \delta(\varepsilon - \varepsilon_q) / M_S$, which is reduced to an energy-independent constant Γ_S in the wide band limit. For simplicity, we set $\phi_S = 0$ in what follows, so that $\Delta_d (\equiv \Gamma_S)$ becomes real. The reduction in the number of the channels gives us a practical advantage in the NRG calculations, because this method works with high accuracy for single-channel systems while the accuracy becomes rather worse for multi-channel systems.

2.2 Effective Anderson Hamiltonian with normal leads

In the NRG method, the normal lead part is transformed into a linear chain after carrying out a standard procedure of the logarithmic discretization.²⁹ Then, a sequence of the Hamiltonians is obtained as

$$\mathcal{H}_{\text{NRG}}^{\text{eff}} = \Lambda^{(N-1)/2} (H_d^0 + H_d^U + H_d^{\text{SC}} + \mathcal{H}_N + \mathcal{H}_{TN}), \quad (6)$$

where

$$\begin{aligned} \mathcal{H}_N + \mathcal{H}_{TN} &= \sum_{n=-1}^{N-1} \sum_{\sigma} t_n \Lambda^{-n/2} \left(f_{n+1\sigma}^\dagger f_{n\sigma} + f_{n\sigma}^\dagger f_{n+1\sigma} \right). \end{aligned} \quad (7)$$

In eq. (7), $f_{-1\sigma} = d_\sigma$, and $f_{n\sigma}$ for $n \geq 0$ is an operator for the conduction electron in the normal lead. The hopping factor t_n is defined by $t_{-1} \equiv \tilde{v} \Lambda^{-1/2}$ for $n = -1$, where

$$\tilde{v} = \sqrt{\frac{2\Gamma_N D A_\Lambda}{\pi}}, \quad A_\Lambda = \frac{1}{2} \left(\frac{1+1/\Lambda}{1-1/\Lambda} \right) \log \Lambda, \quad (8)$$

and for the conduction band ($n \geq 0$),

$$t_n = D \frac{1+1/\Lambda}{2} \frac{1-1/\Lambda^{n+1}}{\sqrt{1-1/\Lambda^{2n+1}} \sqrt{1-1/\Lambda^{2n+3}}}. \quad (9)$$

Here, D is the half-width of the conduction band, and $\Gamma_N (= \pi \sum_k V_N^2 \delta(\varepsilon - \varepsilon_k) |_{\varepsilon = \varepsilon_F} / M_N)$ is the resonance strength between the QD and the normal lead. The factor A_Λ is introduced to compare the discretized model with the original Hamiltonian (3) precisely, and it behaves as $A_\Lambda \rightarrow 1$ in the continuum limit $\Lambda \rightarrow 1$.^{29,35}

In principle, we can carry out the NRG calculation for the Hamiltonian (6). However, we note that H_d^{SC} in eq. (4), which represents the effective onsite superconducting gap at the QD, mixes states with different particle numbers. This means that the eigenstates of the Hamiltonian (6) can not be classified in terms of the total number of electrons. To avoid this inconvenience, we perform the Bogoliubov transformation,³⁶ which is summarized in Appendix B. In the present case the superconducting gap is absent in $\mathcal{H}_N + \mathcal{H}_{TN}$, so that the Hamiltonian (6) can be mapped onto the Anderson model without the

onsite superconducting gap,

$$\begin{aligned} & \Lambda^{-(N-1)/2} \mathcal{H}_{\text{NRG}}^{\text{eff}} \\ &= E_d \left(\sum_{\sigma} \gamma_{-1\sigma}^{\dagger} \gamma_{-1\sigma} - 1 \right) + \frac{U}{2} \left(\sum_{\sigma} \gamma_{-1\sigma}^{\dagger} \gamma_{-1\sigma} - 1 \right)^2 \\ &+ \sum_{n=-1}^{N-1} \sum_{\sigma} t_n \Lambda^{-n/2} (\gamma_{n+1\sigma}^{\dagger} \gamma_{n\sigma} + \text{H.c.}), \end{aligned} \quad (10)$$

where

$$E_d = \sqrt{\left(\varepsilon_d + \frac{U}{2} \right)^2 + \Delta_d^2}. \quad (11)$$

The important point is that the total number of Bogoliubov quasiparticles $\sum_{n=-1}^N \sum_{\sigma} \gamma_{n\sigma}^{\dagger} \gamma_{n\sigma}$ conserves. Moreover, the Hamiltonian (10) is identical to the ordinary Anderson model (without superconductivity). Therefore, the low-energy properties can be described by the local Fermi liquid theory, even though the original model of eq. (6) has the onsite superconducting gap. Equation (10) has been obtained on the assumption that $|\Delta| \rightarrow \infty$. Also for finite $|\Delta|$, the coupling to the normal lead via Γ_N could make the low-lying energy states at $|\varepsilon| \lesssim \min(|\Delta|, T_K)$ be described by the Fermi liquid, where T_K is the Kondo temperature in the case of $\Gamma_S = 0$.

There is another point to be mentioned here. By comparing the first term of the Hamiltonian (10) with H_d^0 in eq. (2), we notice that the parameter $(\varepsilon_d + U/2)$ is replaced by E_d . This means that the Hamiltonian (10) corresponds to the Anderson model with the energy level of the impurity site $\bar{\varepsilon}_d = E_d - U/2$, while the term $(U/2)(n_d - 1)^2$ due to the Coulomb interaction remains unchanged. We discuss the case of $\Gamma_S \neq 0$ ($\Delta_d \neq 0$) in this paper, so that we treat the reduced Hamiltonian (10) with $E_d > 0$ in eq. (11) (so-called asymmetric Anderson model).

2.3 Local Fermi-liquid description

We now introduce the Green function to formulate the density of states (DOS) of the QD. Following eq. (B-11) in Appendix B, we can write down the retarded Green function of the QD, after the Bogoliubov transformation, as follows,

$$G_{d\uparrow, d\uparrow}^r(\varepsilon) = u_d^2 G_{\gamma_{-1\uparrow}, \gamma_{-1\uparrow}}^r(\varepsilon) + v_d^2 \bar{G}_{\gamma_{-1\downarrow}, \gamma_{-1\downarrow}}^r(\varepsilon). \quad (12)$$

Note that the coherent factors u_d, v_d are real because of $\phi_S = 0$. Using eq. (12), the DOS of the QD is given by

$$\begin{aligned} \rho_d(\varepsilon) &= -\frac{1}{\pi} \text{Im} G_{d\uparrow, d\uparrow}^r(\varepsilon) \\ &= -\frac{1}{\pi} \left\{ u_d^2 \text{Im} G_{\gamma_{-1\uparrow}, \gamma_{-1\uparrow}}^r(\varepsilon) + v_d^2 \text{Im} \bar{G}_{\gamma_{-1\downarrow}, \gamma_{-1\downarrow}}^r(\varepsilon) \right\}. \end{aligned} \quad (13)$$

The point we wish to stress is that $G_{\gamma_{-1\uparrow}, \gamma_{-1\uparrow}}^r(\varepsilon)$ and $\bar{G}_{\gamma_{-1\downarrow}, \gamma_{-1\downarrow}}^r(\varepsilon)$ are derived from the generalized Anderson model (10), in which the superconductivity does not show up explicitly.

By using the formula (13), we can describe the Andreev bound states in the QD, which are induced by the

Andreev reflection at the QD-S interface. We here focus on these states around the Fermi energy ($\varepsilon \simeq 0$), where the self-energy due to the Coulomb interaction $\Sigma(\varepsilon)$ is approximately given by $\Sigma(\varepsilon) \simeq \Sigma(0) + \varepsilon \partial \Sigma(\varepsilon) / \partial \varepsilon |_{\varepsilon=0}$. Then, the retarded Green function for electrons after the Bogoliubov transformation reads

$$\begin{aligned} G_{\gamma_{-1\uparrow}, \gamma_{-1\uparrow}}^r(\varepsilon) &= \frac{1}{\varepsilon - E_d + i\Gamma_N - \Sigma(\varepsilon)} \\ &\simeq \frac{z}{\varepsilon - \tilde{E}_d + i\tilde{\Gamma}_N}, \end{aligned} \quad (14)$$

where

$$\tilde{E}_d = z(E_d + \Sigma(0)), \quad \tilde{\Gamma}_N = z\Gamma_N, \quad (15)$$

$$z = \left(1 - \left. \frac{\partial \Sigma(\varepsilon)}{\partial \varepsilon} \right|_{\varepsilon=0} \right)^{-1}. \quad (16)$$

As the retarded Green function for a hole, $\bar{G}_{\gamma_{-1\downarrow}, \gamma_{-1\downarrow}}^r(\varepsilon)$, is given by $\bar{G}_{\gamma_{-1\downarrow}, \gamma_{-1\downarrow}}^r(\varepsilon) = -\left(G_{\gamma_{-1\uparrow}, \gamma_{-1\uparrow}}^r(-\varepsilon) \right)^*$, we end up with the DOS around the Fermi energy,

$$\rho_d(\varepsilon) \simeq \frac{z}{\pi} \left\{ \frac{u_d^2 \tilde{\Gamma}_N}{(\varepsilon - \tilde{E}_d)^2 + \tilde{\Gamma}_N^2} + \frac{v_d^2 \tilde{\Gamma}_N}{(\varepsilon + \tilde{E}_d)^2 + \tilde{\Gamma}_N^2} \right\}. \quad (17)$$

We next consider the transport properties in the small bias regime, which are governed by the Andreev reflection induced inside the superconducting gap. According to Appendix C, the linear conductance $G_{V=0} = dI/dV|_{V=0}$ at zero temperature is given by

$$G_{V=0} = \frac{4e^2}{h} 4 \frac{\Delta_d^2}{E_d^2} \frac{(\tilde{E}_d / \tilde{\Gamma}_N)^2}{\{1 + (\tilde{E}_d / \tilde{\Gamma}_N)^2\}^2}. \quad (18)$$

We see that the conductance is determined by the ratio of the renormalized parameters $\tilde{E}_d / \tilde{\Gamma}_N$, which are obtained from the eigenvalues of the Hamiltonian (10) at the fixed point.³⁷

3. Numerical Results

In this section, we discuss transport properties for the N-QD-S system at zero temperature. As mentioned in the previous section, we assume that the superconducting gap $|\Delta|$ is sufficiently large ($|\Delta| \rightarrow \infty$). In this case the excited states in the continuum outside the superconducting gap can be neglected. It describes a situation where the superconducting gap is much larger than the characteristic energies of the Andreev reflection.

3.1 Influence of the Coulomb interaction U

Let us first discuss how the Coulomb interaction U affects the transport properties at zero temperature. To this end, we explore the detailed properties of the Andreev bound states, which can be obtained from the renormalized parameters computed by means of the NRG method with high accuracy. These renormalized parameters also determine the conductance, so that we can clarify how the conductance is controlled by the Andreev bound states formed around the Fermi energy.

We observe how the Andreev bound states change their characters with the increase of the Coulomb interaction U . As discussed in §2, the local DOS of the QD around

the Fermi energy is given by eq. (17). In particular, in the electron-hole symmetric case ($\varepsilon_d + U/2 = 0$), $E_d = \Gamma_S (\equiv \Delta_d)$ and $u_d^2 = v_d^2 = 1/2$ follow from eqs. (5), (11) and (B-6). Then, the DOS of the QD, $\rho_d(\varepsilon)$, is rewritten as

$$\rho_d(\varepsilon) \simeq \frac{z}{2\pi} \left\{ \frac{\tilde{\Gamma}_N}{(\varepsilon - \tilde{\Gamma}_S)^2 + \tilde{\Gamma}_N^2} + \frac{\tilde{\Gamma}_N}{(\varepsilon + \tilde{\Gamma}_S)^2 + \tilde{\Gamma}_N^2} \right\}, \quad (19)$$

where

$$\tilde{\Gamma}_S = z(\Gamma_S + \Sigma(0)). \quad (20)$$

It is seen from eq. (19) that $\rho_d(\varepsilon)$ in the low-energy region is determined by the renormalized parameters $\tilde{\Gamma}_S$ and $\tilde{\Gamma}_N$. In the noninteracting case ($U = 0$), they are reduced to the bare ones $\tilde{\Gamma}_N = \Gamma_N$ and $\tilde{\Gamma}_S = \Gamma_S$. In this case, the Andreev bound states are formed at $\varepsilon = \pm\Gamma_S$, which are broadened (finite width Γ_N) by the coupling between the QD and the normal lead, as schematically shown in Fig. 1(a). We shall refer to these Andreev bound states with

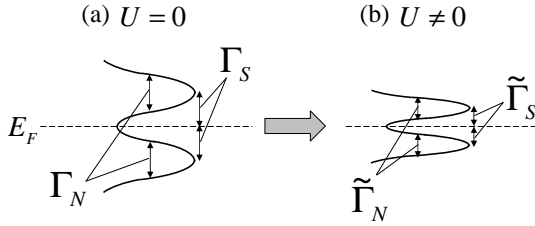


Fig. 1. Andreev resonances around the Fermi energy ($E_F = 0$) in the symmetric case ($\varepsilon_d + U/2 = 0$).

finite widths as the Andreev resonances in the following. Here we would like to comment on Γ_S , which gives the position of the Andreev resonances shown in Fig. 1(a). The Andreev reflection at the QD-S interface gives rise to the superconducting correlation in the QD. Taking into account eqs. (4) and (5), in the case of $|\Delta| \rightarrow \infty$, we see the amplitude of the superconducting correlation in the QD is given by the resonance strength $\Gamma_S (\equiv \Delta_d)$. Then, Γ_S becomes a parameter indicating the strength of the Andreev reflection at the QD-S interface, while it originally represents the position of the Andreev resonances in the QD. When the Coulomb interaction U is introduced, the effective tunneling of electrons between the QD and the leads is modified, so that the Andreev resonances are renormalized. Namely, the position and the width of these resonances, which correspond to the renormalized parameters $\tilde{\Gamma}_S$ and $\tilde{\Gamma}_N$ respectively, become smaller with the increase of U (see Fig. 1(b)). Note that when the effect of the Coulomb interaction U is included, the strength of the Andreev reflection at the QD-S interface is given by $\tilde{\Gamma}_S$ instead of Γ_S . Since we are concerned with the DOS around the Fermi energy, the Andreev resonances away from the Fermi energy are not shown in Fig. 1(b). The overall structure including the high energy region can be found in the literature.^{16, 19–21, 25}

To observe the formation of the Andreev resonances in our model, we calculate the renormalized parameters $\tilde{\Gamma}_S$

and $\tilde{\Gamma}_N$. Figure 2(a) shows the renormalized parameters $\tilde{\Gamma}_N$ and $\tilde{\Gamma}_S$ as a function of the Coulomb interaction U for $\Gamma_S = \Gamma_N$, where the parameters $\tilde{\Gamma}_{N(S)}$ are normalized by the bare resonance strength, Γ_N . As shown in Fig.

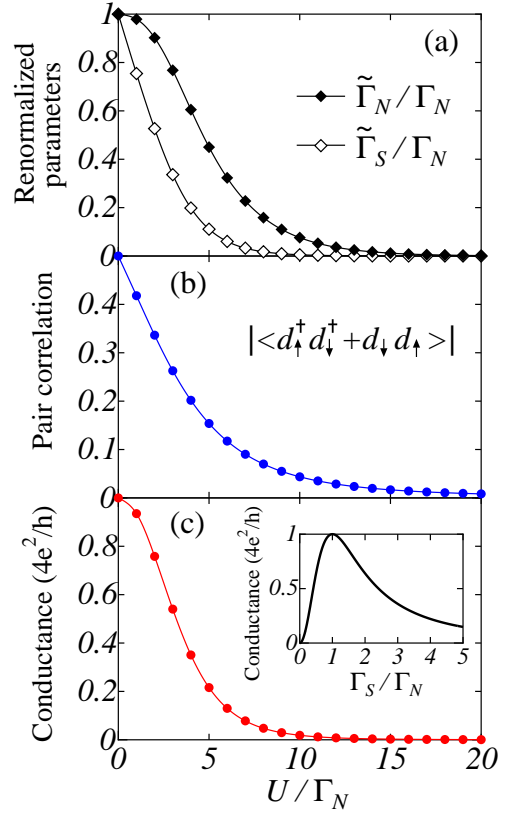


Fig. 2. (Color online) (a) Renormalized parameters $\tilde{\Gamma}_S$ and $\tilde{\Gamma}_N$, (b) expectation value of the pair correlation in the QD and (c) linear conductance as a function of the Coulomb interaction U for $\Gamma_S = \Gamma_N$ in the symmetric case ($\varepsilon_d + U/2 = 0$). $\tilde{\Gamma}_{N(S)}$ and U are normalized by the bare resonance strength, Γ_N . The NRG calculations have been carried out for $\Lambda = 3.0$ and $\Gamma_N/D = 1.0 \times 10^{-3}$. Inset of (c): Conductance in the noninteracting case ($U = 0$) as a function of the ratio Γ_S/Γ_N , where we set $\varepsilon_d = 0$.

2(a), both of $\tilde{\Gamma}_S$ and $\tilde{\Gamma}_N$ decrease monotonically with the increase of U . The decrease of $\tilde{\Gamma}_N$ signals a crossover from the charge-fluctuation regime to the Kondo regime, as is the case for general N-QD-N systems. On the other hand, the decrease of $\tilde{\Gamma}_S$ results in the suppression of the Andreev reflection at the QD-S interface, implying that the superconducting correlation is suppressed in the QD. To confirm this implication, we also calculate the expectation value of the pair correlation in the QD, which is given by

$$\langle d_{\uparrow}^{\dagger} d_{\downarrow}^{\dagger} + d_{\downarrow} d_{\uparrow} \rangle = -\frac{2}{\pi} \tan^{-1}(\tilde{\Gamma}_S/\tilde{\Gamma}_N). \quad (21)$$

Note that the sign of $\langle d_{\uparrow}^{\dagger} d_{\downarrow}^{\dagger} + d_{\downarrow} d_{\uparrow} \rangle$ depends on the definition of the superconducting gap Δ in H_S : namely, $\langle d_{\uparrow}^{\dagger} d_{\downarrow}^{\dagger} + d_{\downarrow} d_{\uparrow} \rangle$ becomes negative because the second term in the right hand side of eq. (2) is assumed to be positive. As shown in Fig. 2(b), we see that the absolute value $|\langle d_{\uparrow}^{\dagger} d_{\downarrow}^{\dagger} + d_{\downarrow} d_{\uparrow} \rangle|$ approaches 0 with the increase of U

and/or $\tilde{\Gamma}_S$ in Fig. 2(a). The Andreev resonances around the Fermi energy are thus renormalized with the increase of U , as shown in Fig. 1. It is to be noticed that in the large U region where the Kondo effect is dominant, these two resonances merge around the Fermi energy, forming a single sharp Kondo resonance, in accordance with refs. 16, 19–21 and 25. This is indeed seen from the tendency that $\tilde{\Gamma}_S$ decreases more rapidly than $\tilde{\Gamma}_N$ in Fig. 2(a).

We next discuss how the conductance changes with the increase of U . In the symmetric case ($\varepsilon_d + U/2 = 0$), the conductance of eq. (18) is rewritten as

$$G_{V=0}^{\varepsilon_d + \frac{U}{2} = 0} = \frac{4e^2}{h} \frac{4(\tilde{\Gamma}_S/\tilde{\Gamma}_N)^2}{\{1 + (\tilde{\Gamma}_S/\tilde{\Gamma}_N)^2\}^2}. \quad (22)$$

The conductance of eq. (22) is a function of the ratio $\tilde{\Gamma}_S/\tilde{\Gamma}_N$ and has a maximum at $\tilde{\Gamma}_S/\tilde{\Gamma}_N = 1$, as pointed out in the previous studies.^{17,21} Here, we would like to mention the relation between the conductance and the Andreev resonances shown in Fig. 1. In the case of $\tilde{\Gamma}_S/\tilde{\Gamma}_N = 1$, which corresponds to the condition for the maximum of the conductance, the distance of the Andreev resonances measured from the Fermi energy ($\tilde{\Gamma}_S$) is equal to the width of these resonances ($\tilde{\Gamma}_N$). We also consider the case of $\tilde{\Gamma}_S/\tilde{\Gamma}_N \neq 1$. When $\tilde{\Gamma}_S/\tilde{\Gamma}_N > 1$, the distance $\tilde{\Gamma}_S$ becomes larger than the width $\tilde{\Gamma}_N$. Then, the DOS of the QD around the Fermi energy gets smaller, which results in the decrease of the conductance. On the other hand, when $\tilde{\Gamma}_S/\tilde{\Gamma}_N < 1$, the Andreev resonances get closer to the Fermi energy, which leads to the enhancement of the DOS around the Fermi energy. At the same time, however, this means that the transport due to the Andreev reflection is suppressed, so that the conductance decreases as well as the case of $\tilde{\Gamma}_S/\tilde{\Gamma}_N > 1$.

Figure 2(c) shows the conductance computed as a function of the Coulomb interaction U for $\Gamma_S = \Gamma_N$. For reference, we also plot the conductance in the noninteracting case ($U = 0$) as a function of the ratio Γ_S/Γ_N (inset of Fig. 2(c)), which is given by replacing $\tilde{\Gamma}_S/\tilde{\Gamma}_N$ in eq. (22) with Γ_S/Γ_N . From the inset, we see that the conductance for $U = 0$ has the maximum at $\Gamma_S/\Gamma_N = 1$, where the couplings to normal and superconducting leads have the same amplitude. In this case, the maximum value of the conductance reaches the unitary limit $4e^2/h$ because of the electron-hole symmetry. With the increase of U , the conductance decreases monotonically from $4e^2/h$, as shown in Fig. 2(c). This behavior is in agreement with Cuevas *et al.*'s results, where they treated a system with a finite gap Δ of the superconducting lead.²¹ As stated in ref. 21, this is due to the reduction of $\tilde{\Gamma}_S/\tilde{\Gamma}_N$, which corresponds to the case of $\tilde{\Gamma}_S/\tilde{\Gamma}_N < 1$ stated above. Similar behavior of monotonic reduction is observed for smaller Γ_S ($\Gamma_S/\Gamma_N < 1$).

Note, however, that somewhat different behavior appears in the region of $\Gamma_S/\Gamma_N > 1$. Figure 3 shows similar plots of the renormalized parameters and the conductance for $\Gamma_S/\Gamma_N = 5$. Let us focus on the small U region in Fig. 3(a) and (b). In this region, $\tilde{\Gamma}_S$ decreases monotonically, which reduces the absolute value $|\langle d_\uparrow^\dagger d_\downarrow^\dagger + d_\downarrow d_\uparrow \rangle|$, as is the case of $\Gamma_S/\Gamma_N = 1$. On the other

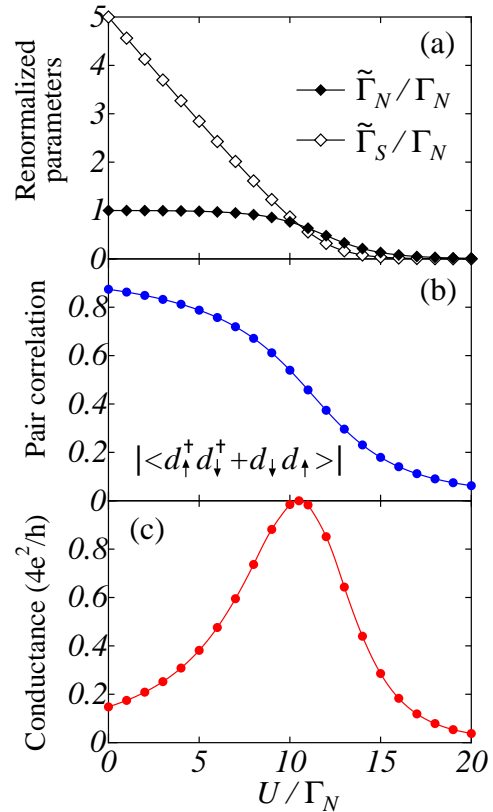


Fig. 3. (Color online) (a) Renormalized parameters $\tilde{\Gamma}_S$ and $\tilde{\Gamma}_N$, (b) expectation value of the pair correlation in the QD and (c) linear conductance as a function of the Coulomb interaction U for $\Gamma_S/\Gamma_N = 5$. The other parameters are the same as in Fig. 2.

hand, $\tilde{\Gamma}_N$ remains almost unchanged unlike the case of $\Gamma_S/\Gamma_N = 1$. This result indicates that the position of the Andreev resonances approaches the Fermi energy, keeping its resonance width unchanged. However, when the value of $\tilde{\Gamma}_S$ gets close to that of $\tilde{\Gamma}_N$, $\tilde{\Gamma}_N$ also begins to decrease. For larger U , both $\tilde{\Gamma}_S$ and $\tilde{\Gamma}_N$ approach 0, as is the case of $\Gamma_S/\Gamma_N = 1$. Comparing $\tilde{\Gamma}_S$ and $\tilde{\Gamma}_N$ in Fig. 3(a) with the conductance shown in Fig. 3(c), we see that the conductance has the maximum when the condition $\tilde{\Gamma}_S = \tilde{\Gamma}_N$ is satisfied.

Summarizing the above results, we can say that the conductance shows the characteristic U -dependence accompanied by the maximum structure, around which the strength of two effective resonances is exchanged: we have $\tilde{\Gamma}_S > \tilde{\Gamma}_N$ in the small U region ($U/\Gamma_N < 10$), while $\tilde{\Gamma}_S < \tilde{\Gamma}_N$ in the large U region ($U/\Gamma_N > 10$). In the following, we demonstrate that the maximum of the conductance characterizes a crossover between the two distinct singlet regions where either the superconducting correlation or the Kondo correlation is dominant.

3.2 Implications of the conductance maximum

To discuss the condition that the conductance takes the maximum value in more detail, we would like to observe how the conductance changes as a function of the resonance strength Γ_S that gives a measure of the superconducting correlation in the QD, as has been done in ref. 21. We find it more instructive to summarize our

results in two-dimensional plots in the plane of Γ_S and U , which indeed allows us to elucidate how the electron correlations affect the conductance maximum.

Figure 4 (a) is the color-scale representation of the conductance as a function of U/Γ_N and Γ_S/Γ_N . We also show the enlarged picture in small U and Γ_S region in Fig. 4(b). As shown in Fig. 4(b), the conductance takes

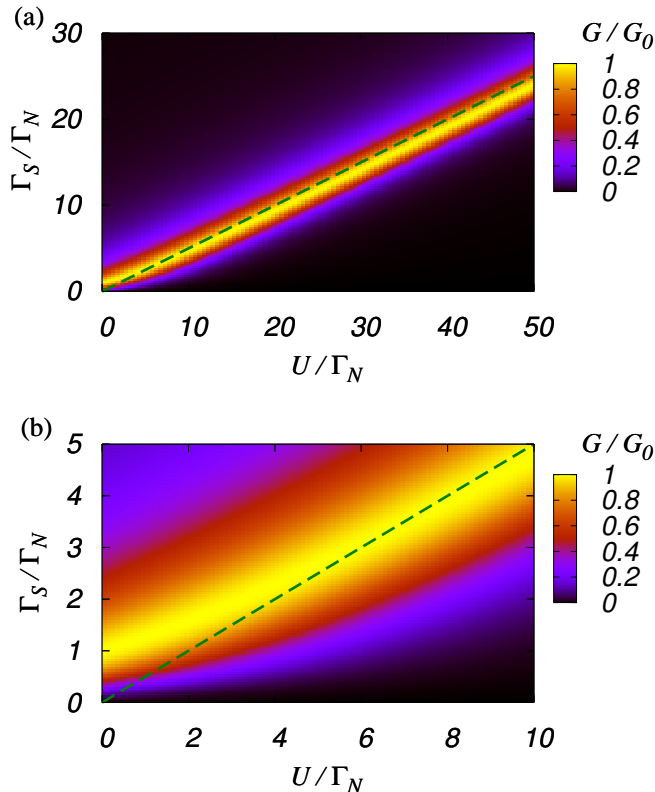


Fig. 4. (Color online) (a) Color-scale representation of the conductance G/G_0 , where $G_0 = 4e^2/h$, as a function of U/Γ_N and Γ_S/Γ_N . The dashed line, $\Gamma_S = U/2$, represents the boundary of the singlet-doublet transition for $\Gamma_N = 0$. (b) Enlarged picture in the region with small U/Γ_N and Γ_S/Γ_N .

the maximum at $\Gamma_S/\Gamma_N = 1$ when $U/\Gamma_N = 0$, in accordance with the inset of Fig. 2. As U/Γ_N increases, the value of Γ_S/Γ_N giving the maximum of the conductance increases linearly along the line of $\Gamma_S = U/2$ (see Fig. 4). As mentioned above, the maximum of the conductance reaches the unitary limit ($G_0 = 4e^2/h$) because of the electron-hole symmetry. For instance, around $U/\Gamma_N = 10$ and $\Gamma_S/\Gamma_N = 5$, the conductance reaches the unitary limit, as already shown in Fig. 3(c).

Here we consider the physical implication of $\Gamma_S = U/2$, which coincides with the condition that the conductance reaches the unitary limit for large values of Γ_S/Γ_N and U/Γ_N . To this end, let us examine the limit of $\Gamma_N \rightarrow 0$. When $\Gamma_N = 0$, the QD is disconnected from the normal lead, and only connected to the superconducting lead (QD-S). Recall here that the QD-S system is equivalent to a magnetic impurity model embedded in a superconductor, which has been studied for dilute magnetic alloys.^{38–41} As discussed in refs. 38–41, the ground state of the QD-S system is a nonmagnetic singlet or a

magnetic doublet. Specifically in the limit of $|\Delta| \rightarrow \infty$, the ground state only depends on the ratio of Γ_S/U . Namely, the ground state is a superconducting spin-singlet state for $\Gamma_S/U > 0.5$ or a spin-doublet state for $\Gamma_S/U < 0.5$. A transition between these ground states occurs at $\Gamma_S/U = 0.5$.

We now observe what happens for finite Γ_N . When the coupling between the QD and the normal lead is introduced, conduction electrons in the normal lead screen the free spin moment to form the Kondo singlet state in the region of $\Gamma_S/U < 0.5$. Therefore, the ground state of the N-QD-S system is always singlet. There are, however, two distinct singlets, i.e. one with superconducting-singlet character for $\Gamma_S/U > 0.5$ and the other with Kondo-singlet character for $\Gamma_S/U < 0.5$. From the above discussion, we see that the maximum of the conductance in Fig. 4 for large values of Γ_S/Γ_N and U/Γ_N clearly characterizes the crossover between these two different spin-singlet states. We have drawn this conclusion on the assumption that the gap is sufficiently large ($|\Delta| \rightarrow \infty$). We believe that this conclusion also holds for an N-QD-S system with a finite gap Δ of the superconducting lead, though the onset of the transition of the ground state for $\Gamma_N = 0$ depends also on Δ .^{32,33}

Before closing this subsection, we display the conductance in Fig. 5 in a slightly different way to make the comparison with experiments easier; it is plotted as a function of the ratio Γ_S/U for several values of Γ_N/U , which are both controllable by changing the voltage between the QD and the leads experimentally.^{2,3} From

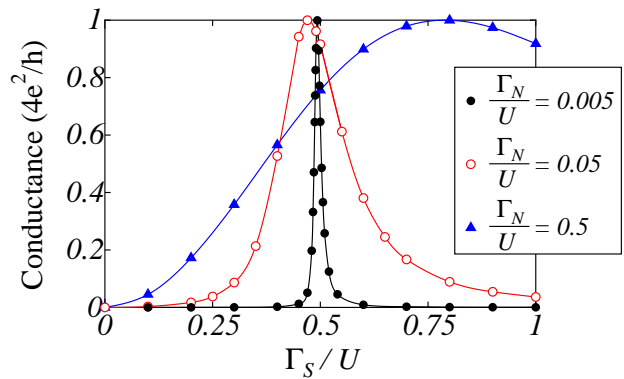


Fig. 5. (Color online) Conductance as a function of the ratio Γ_S/U for several values of Γ_N/U , where the Coulomb interaction is fixed as $U/D = 2.0 \times 10^{-2}$.

Fig. 5, we see that as Γ_N/U gets smaller, the peak structure becomes sharper and its position approaches $\Gamma_S/U = 0.5$. Thus, the peak structure in the conductance for $\Gamma_N/U = 0.05$ and 0.005 in Fig. 5 clearly characterizes the crossover between the superconducting and Kondo spin-singlet states, as discussed above. On the other hand, as Γ_N/U becomes larger, the peak structure is somewhat broadened and its position shifts toward $\Gamma_S/U > 0.5$, as shown for $\Gamma_N/U = 0.5$ in Fig. 5. Note here that the increase of Γ_N/U enhances charge fluctuations in the QD, making the Kondo correlation

weak. Therefore, the crossover between the superconducting and Kondo singlet states becomes smeared, and accordingly the position of the conductance maximum deviates from $\Gamma_S/U = 0.5$.

3.3 Away from the symmetric case

Finally, we discuss the conductance as a function of the energy level in the QD, ε_d , away from the electron-hole symmetric case ($\varepsilon_d + U/2 \neq 0$). Note that the energy level in the QD can be changed by the gate-voltage control. A deviation from the electron-hole symmetric case is represented by H_d^0 in eq. (2), as stated in §2. In this case, the position of the Andreev resonances is given by \tilde{E}_d in eq. (15) instead of $\tilde{\Gamma}_S$. Following the way outlined in the symmetric case, we discuss the characteristics of the conductance in connection with the ground-state nature of the system.

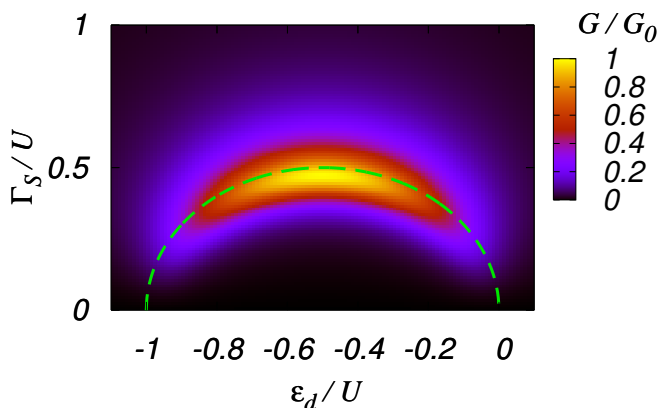


Fig. 6. (Color online) Color-scale representation of the conductance G/G_0 ($G_0 = 4e^2/h$) as a function of ε_d/U and Γ_S/U . In this calculation, we set $\Gamma_N/U = 0.05$ and $U/D = 2.0 \times 10^{-2}$. The dashed line is $\{(\varepsilon_d/U + 1/2)^2 + (\Gamma_S/U)^2\}^{1/2} = 1/2$, which gives the boundary of the singlet-doublet transition for $\Gamma_N = 0$.

In Fig. 6 we show the conductance in the color-scale representation as a function of ε_d/U and Γ_S/U . We also draw a half circle given by $\{(\varepsilon_d/U + 1/2)^2 + (\Gamma_S/U)^2\}^{1/2} = 1/2$, which denotes the boundary of the singlet-doublet transition for $\Gamma_N = 0$, which is replaced with the Kondo spin-singlet region in the presence of any finite Γ_N . On the other hand, the outside is the superconducting spin-singlet region. From Fig. 6, we see that the conductance for $\Gamma_S/U < 0.5$ has large values along the half circle. This means that the conductance as a function of ε_d has two peaks.²¹ Note here that a deviation from the electron-hole symmetric case ($\varepsilon_d/U \neq -0.5$) makes the Kondo correlation weaker. Therefore, the two-peak structure of the conductance for $\Gamma_S/U < 0.5$ indicates the crossover of superconducting-Kondo-superconducting singlet states. On the other hand, for $\Gamma_S/U > 0.5$, the ground state is the superconducting singlet state for any values of ε_d/U . As seen in eqs. (11) and (15), a deviation from the symmetric case drives the position of the Andreev resonances

(\tilde{E}_d) away from the Fermi energy. In the superconducting singlet region ($\Gamma_S/U > 0.5$), $\tilde{E}_d/\tilde{\Gamma}_N > 1$ is satisfied, so that the deviation leads to the reduction of the conductance, as is the case of $\tilde{\Gamma}_S/\tilde{\Gamma}_N > 1$ in the symmetric case. Thus, the conductance as a function of ε_d has a single maximum at $\varepsilon_d/U = -0.5$, although this peak is not a sign of the crossover between two singlet states unlike the peaks for $\Gamma_S/U < 0.5$.

4. Summary

We have investigated transport properties of an N-QD-S system using the NRG method. Especially, we have focused on the limiting case of $|\Delta| \rightarrow \infty$ with particular emphasis on the Andreev reflection which arises inside the superconducting gap. Adapting the Bogoliubov transformation to the simplified model, we have first demonstrated that our system with superconductivity can be mapped on an effective Anderson impurity model without superconductivity, which enables us to describe the low-energy properties in terms of the local Fermi liquid theory.

To clarify the influence of the Coulomb interaction on the transport due to the Andreev reflection, we have calculated the conductance as a function of the Coulomb interaction U . For the ratio $\Gamma_S/\Gamma_N > 1$, the conductance has the maximum in its U -dependence while for $\Gamma_S/\Gamma_N \leq 1$ it decreases monotonically, which is in accordance with Cuevas *et al.*'s results. We have also calculated the renormalized parameters to discuss the conductance in connection with the Andreev resonances around the Fermi energy. Through the analysis using the renormalized parameters, we have found that the maximum of the conductance gives an indication of the crossover between two distinct types of singlet ground states. To observe the nature of the crossover in detail, we have studied the transport properties by focusing on the changes of the Coulomb interaction U and the resonance strength Γ_S . In particular, starting from the special case with $\Gamma_N = 0$, i.e. the QD system only coupled to the superconducting lead, we have shown that the conductance maximum clearly characterizes the crossover between the Kondo singlet state and the superconducting singlet state.

It has been further elucidated that the gate-voltage dependence of the conductance shows different behavior depending on the value of Γ_S ; there are two peaks in the gate-voltage dependence characterizing the crossover of superconducting-Kondo-superconducting singlet regions for $\Gamma_S/U < 0.5$, whereas only a single maximum appears in the superconducting singlet region for $\Gamma_S/U > 0.5$.

In this paper, we have clarified several characteristic transport properties on the assumption that the superconducting gap is sufficiently large. Nevertheless we believe that our main conclusion, *i.e.* the conductance maximum clearly characterizes the crossover between two distinct types of singlet ground states, holds even for general N-QD-S systems with a finite gap Δ . In this case, however, the crossover between two distinct types of singlet states depends also on Δ , as stated in §3. In near future, we expect that the characteristic maximum structure found in the conductance due to the Andreev reflection

tion will be observed experimentally.

Acknowledgment

We would like to thank Y. Nisikawa and T. Suzuki for valuable discussions. A part of computations was done at the Supercomputer Center at the Institute for Solid State Physics, University of Tokyo. The work was partly supported by a Grant-in-Aid from the Ministry of Education, Culture, Sports, Science and Technology of Japan. Y. Tanaka is supported by JSPS Research Fellowships for Young Scientists. A. Oguri is supported by a Grant-in-Aid from JSPS.

Appendix A: Hamiltonian at $|\Delta| \rightarrow \infty$

We explain how the Hamiltonian (1) can be reduced to an effective single-channel Hamiltonian (3) in the limit of $|\Delta| \rightarrow \infty$. For this purpose, we consider the Green function of the QD in the 2×2 Nambu representation, which takes the form

$$\begin{aligned} \mathbf{G}_{d,d}(t-t') &= -i \begin{pmatrix} \langle T d_{\uparrow}(t) d_{\uparrow}^{\dagger}(t') \rangle & \langle T d_{\uparrow}(t) d_{\downarrow}(t') \rangle \\ \langle T d_{\downarrow}^{\dagger}(t) d_{\uparrow}^{\dagger}(t') \rangle & \langle T d_{\downarrow}^{\dagger}(t) d_{\downarrow}(t') \rangle \end{pmatrix} \\ &= \begin{pmatrix} G_{d_{\uparrow},d_{\uparrow}}(t-t') & \bar{F}_{d_{\uparrow},d_{\downarrow}}(t-t') \\ F_{d_{\downarrow},d_{\uparrow}}(t-t') & \bar{G}_{d_{\downarrow},d_{\downarrow}}(t-t') \end{pmatrix}. \end{aligned} \quad (\text{A.1})$$

We perform the Fourier transformation of the retarded (advanced) Green function for eq. (A.1). From the Dyson equation, we have

$$\left(\varepsilon \mathbf{I} - \varepsilon_d \boldsymbol{\tau}_3 - \boldsymbol{\Sigma}^{r(a)}(\varepsilon) \right) \mathbf{G}_{d,d}^{r(a)}(\varepsilon) = \mathbf{I}. \quad (\text{A.2})$$

In the interacting case, the self-energy $\boldsymbol{\Sigma}^{r(a)}(\varepsilon)$ can be classified into two parts

$$\boldsymbol{\Sigma}^{r(a)}(\varepsilon) = \boldsymbol{\Sigma}_0^{r(a)}(\varepsilon) + \boldsymbol{\Sigma}_U^{r(a)}(\varepsilon), \quad (\text{A.3})$$

where $\boldsymbol{\Sigma}_0^{r(a)}(\varepsilon)$ is the self-energy due to the mixing between the QD and the leads, and $\boldsymbol{\Sigma}_U^{r(a)}(\varepsilon)$ is due to the Coulomb interaction. The exact expression for $\boldsymbol{\Sigma}_0^r(= (\boldsymbol{\Sigma}_0^a)^{\dagger})$ is written down as

$$\boldsymbol{\Sigma}_0^r(\varepsilon) = \begin{pmatrix} -i(\Gamma_N + \Gamma_S \beta(\varepsilon)) & i\Gamma_S \beta(\varepsilon) \frac{\Delta}{\varepsilon} \\ i\Gamma_S \beta(\varepsilon) \frac{\Delta}{\varepsilon} & -i(\Gamma_N + \Gamma_S \beta(\varepsilon)) \end{pmatrix}, \quad (\text{A.4})$$

where

$$\beta(\varepsilon) = \frac{|\varepsilon| \theta(|\varepsilon| - |\Delta|)}{\sqrt{\varepsilon^2 - |\Delta|^2}} + \frac{\varepsilon \theta(|\Delta| - |\varepsilon|)}{i\sqrt{|\Delta|^2 - \varepsilon^2}}. \quad (\text{A.5})$$

Here, we consider the case that the superconducting gap is sufficiently large, i.e. the limit of $|\Delta| \rightarrow \infty$. In this limit, taking into account $\beta(\varepsilon) \rightarrow \frac{\varepsilon}{i\sqrt{|\Delta|^2 - \varepsilon^2}}$, $\boldsymbol{\Sigma}_0^r(\varepsilon)$ is reduced to

$$\lim_{|\Delta| \rightarrow \infty} \boldsymbol{\Sigma}_0^r(\varepsilon) = \begin{pmatrix} -i\Gamma_N & \Gamma_S e^{i\phi_S} \\ \Gamma_S e^{-i\phi_S} & -i\Gamma_N \end{pmatrix}. \quad (\text{A.6})$$

We note that the off-diagonal element in eq. (A.6) can be regarded as a static superconducting gap induced at the QD, and its amplitude is given by the resonance strength Γ_S . Therefore, in the limit of $|\Delta| \rightarrow \infty$ the information

about the superconducting lead can be included through the off-diagonal term of the Green function of the QD. This enables us to rewrite the Hamiltonian (1) to an effective single-channel Hamiltonian with an extra superconducting gap at the QD in eqs. (3) and (4).

Appendix B: Bogoliubov transformation

We perform the Bogoliubov transformation for the Hamiltonian (6). Using the Nambu representation, $H_d^0 + H_d^{\text{SC}}$ and $\mathcal{H}_N + \mathcal{H}_{TN}$ in the Hamiltonian (6) are rewritten as,

$$H_d^0 + H_d^{\text{SC}} = \psi_{f,-1}^{\dagger} \begin{pmatrix} \xi_d & \Delta_d \\ \Delta_d^* & -\xi_d \end{pmatrix} \psi_{f,-1}, \quad (\text{B.1})$$

$$\mathcal{H}_N + \mathcal{H}_{TN} = \sum_{n=-1}^{N-1} t_n \Lambda^{-n/2} \left(\psi_{f,n+1}^{\dagger} \psi_{f,n} + \psi_{f,n}^{\dagger} \psi_{f,n+1} \right), \quad (\text{B.2})$$

where

$$\psi_{f,n} = \begin{pmatrix} f_{n\uparrow} \\ (-1)^{n-1} f_{n\downarrow} \end{pmatrix}. \quad (\text{B.3})$$

In eq. (B.1), $\xi_d = \varepsilon_d + U/2$ and $f_{-1\sigma} = d_{\sigma}$. For eqs. (B.1) and (B.2), we carry out the Bogoliubov transformation,

$$\psi_{\gamma,n} = \mathbf{U}_d^{\dagger} \psi_{f,n}, \quad (\text{B.4})$$

where

$$\psi_{\gamma,n} = \begin{pmatrix} \gamma_{n\uparrow} \\ (-1)^{n-1} \gamma_{n\downarrow} \end{pmatrix}, \quad \mathbf{U}_d = \begin{pmatrix} u_d & -v_d^* \\ v_d & u_d^* \end{pmatrix}, \quad (\text{B.5})$$

$$|u_d|^2 = \frac{1}{2} \left(1 + \frac{\xi_d}{E_d} \right), \quad |v_d|^2 = \frac{1}{2} \left(1 - \frac{\xi_d}{E_d} \right), \quad (\text{B.6})$$

$$E_d = \sqrt{\xi_d^2 + |\Delta_d|^2}. \quad (\text{B.7})$$

As a result, each term of the Hamiltonian $\mathcal{H}_{\text{NRG}}^{\text{eff}}$ can be transformed as follows,

$$H_d^0 + H_d^{\text{SC}} = E_d \left(\sum_{\sigma} \gamma_{-1\sigma}^{\dagger} \gamma_{-1\sigma} - 1 \right), \quad (\text{B.8})$$

$$H_d^U = \frac{U}{2} \left(\sum_{\sigma} \gamma_{-1\sigma}^{\dagger} \gamma_{-1\sigma} - 1 \right)^2, \quad (\text{B.9})$$

$$\mathcal{H}_N + \mathcal{H}_{TN} = \sum_{n=-1}^{N-1} \sum_{\sigma} t_n \Lambda^{-n/2} \left(\gamma_{n+1\sigma}^{\dagger} \gamma_{n\sigma} + \text{H.c.} \right). \quad (\text{B.10})$$

eqs. (B.8), (B.9) and (B.10) give the Hamiltonian (10). We should notice that H_d^U remains unchanged under the Bogoliubov transformation.

We finally show how the Green function of the QD is transformed via the Bogoliubov transformation. Applying the Bogoliubov transformation of eq. (B.4) to the Fourier transformation of eq. (A.1),

$$\mathbf{G}_{d,d}(\varepsilon) = \mathbf{U}_d \mathbf{G}_{\gamma_{-1},\gamma_{-1}}(\varepsilon) \mathbf{U}_d^{\dagger}, \quad (\text{B.11})$$

where the Green function $\mathbf{G}_{\gamma_{-1},\gamma_{-1}}(\varepsilon)$ is for the Hamiltonian after the Bogoliubov transformation. Therefore, we

end up with $\mathbf{G}_{\gamma_{-1},\gamma_{-1}}(\varepsilon)$ without off-diagonal elements,

$$\mathbf{G}_{\gamma_{-1},\gamma_{-1}}(\varepsilon) = \begin{pmatrix} G_{\gamma_{-1}\uparrow,\gamma_{-1}\uparrow}(\varepsilon) & 0 \\ 0 & \bar{G}_{\gamma_{-1}\downarrow,\gamma_{-1}\downarrow}(\varepsilon) \end{pmatrix}. \quad (\text{B}\cdot 12)$$

Appendix C: Derivation of eq. (18)

By applying the Landauer formula, we derive the linear conductance $dI/dV|_{V=0}$. The current from the normal lead to the QD is given in terms of the Nambu representation^{12,16}

$$I = \frac{2e}{h} \int d\varepsilon (i\Gamma_N) [\mathbf{G}_{d,d}^r(\varepsilon)\mathbf{\Omega}(\varepsilon)\mathbf{G}_{d,d}^a(\varepsilon) - 2i(1-2f_N)\text{Im}\mathbf{G}_{d,d}^r(\varepsilon)]_{11}. \quad (\text{C}\cdot 1)$$

The subscript 11 means the (1,1) element of the matrix. $\mathbf{\Omega}(\varepsilon)$ is the self-energy given by $\mathbf{\Omega}(\varepsilon) = -\mathbf{\Sigma}^<(\varepsilon) - \mathbf{\Sigma}^>(\varepsilon)$, where $\mathbf{\Sigma}^<(>)(\varepsilon)$ is the lesser (greater) self-energy for the QD. $f_N = f(\varepsilon - eV)$, where $f(\varepsilon)$ is the Fermi distribution function. Similarly to $\mathbf{\Sigma}^{r(a)}(\varepsilon)$ in eq. (A·3), the self-energy $\mathbf{\Omega}(\varepsilon)$ can be classified into two parts,

$$\mathbf{\Omega}(\varepsilon) = \mathbf{\Omega}_0(\varepsilon) + \mathbf{\Omega}_U(\varepsilon), \quad (\text{C}\cdot 2)$$

where $\mathbf{\Omega}_0(\varepsilon)$ ($\mathbf{\Omega}_U(\varepsilon)$) is due to the mixing between the QD and the leads (Coulomb interaction). Using eq. (C·1), we consider the linear conductance $G_{V=0} = dI/dV|_{V=0}$ at zero temperature. It should be noted that $\text{Im}\mathbf{\Sigma}_U^r(0)|_{V=0} = 0$ at zero temperature, so that the term including $\mathbf{\Omega}_U(\varepsilon)$ vanishes. Namely, assuming that $\text{Im}\mathbf{\Sigma}_U^r(0)|_{V=0} = 0$ and $\mathbf{\Omega}_U(0)|_{V=0} = 0$ at zero temperature, correlation effects on $G_{V=0}$ at zero temperature enter through $\text{Re}\mathbf{\Sigma}_U^r(0)|_{V=0}$. On the other hand, the exact formula for $\mathbf{\Omega}_0(\varepsilon)$ is given by

$$\mathbf{\Omega}_0(\varepsilon) = -2i \begin{pmatrix} (1-2f_N)\Gamma_N + (1-2f_S)\Gamma_S\tilde{\rho}_S(\varepsilon) & \\ -(1-2f_S)\Gamma_S\tilde{\rho}_S(\varepsilon)\frac{\Delta}{\varepsilon} & \\ & -(1-2f_S)\Gamma_S\tilde{\rho}_S(\varepsilon)\frac{\Delta}{\varepsilon} \\ (1-2\bar{f}_N)\Gamma_N + (1-2f_S)\Gamma_S\tilde{\rho}_S(\varepsilon) & \end{pmatrix}, \quad (\text{C}\cdot 3)$$

where $f_S = f(\varepsilon)$, $\bar{f}_N = f(\varepsilon + eV)$ and $\tilde{\rho}_S(\varepsilon) = \frac{|\varepsilon|\theta(|\varepsilon|-\Delta)}{\sqrt{\varepsilon^2-\Delta^2}}$. Using the retarded (advanced) Green function in eq. (A·2) together with eq. (C·3), we obtain the linear conductance at the zero temperature as,

$$G_{V=0} = \frac{4e^2}{h} 4\Gamma_N^2 |\bar{F}_{d\uparrow,d\downarrow}^r(0)|^2. \quad (\text{C}\cdot 4)$$

As shown in eq. (A·1), $\bar{F}_{d\uparrow,d\downarrow}^r(\varepsilon)$ is the (1,2) element of $\mathbf{G}_{d,d}^r(\varepsilon)$. Using $G_{\gamma_{-1}\uparrow,\gamma_{-1}\uparrow}^r(\varepsilon)$ in eq. (14) and eqs. (B·5), (B·11) and (B·12), we can rewrite $\bar{F}_{d\uparrow,d\downarrow}^r(\varepsilon)$ around the Fermi energy as

$$\begin{aligned} \bar{F}_{d\uparrow,d\downarrow}^r(\varepsilon) &= u_d v_d \left(G_{\gamma_{-1}\uparrow,\gamma_{-1}\uparrow}^r(\varepsilon) - \bar{G}_{\gamma_{-1}\downarrow,\gamma_{-1}\downarrow}^r(\varepsilon) \right) \\ &\simeq u_d v_d \left(\frac{z}{\varepsilon - \tilde{E}_d + i\tilde{\Gamma}_N} - \frac{z}{\varepsilon + \tilde{E}_d + i\tilde{\Gamma}_N} \right). \end{aligned} \quad (\text{C}\cdot 5)$$

Substituting eq. (C·5) into eq. (C·4), we have

$$G_{V=0} = \frac{4e^2}{h} 4 \frac{\Delta_d^2}{E_d^2} \frac{\tilde{\Gamma}_N^2 \tilde{E}_d^2}{(\tilde{\Gamma}_N^2 + \tilde{E}_d^2)^2}. \quad (\text{C}\cdot 6)$$

Note that the factor Δ_d^2/E_d^2 coming from u_d and v_d in eq. (B·6) is not renormalized by the Coulomb interaction.

- 1) For review, see L. P. Kouwenhoven, D. G. Austing, and S. Tarucha: Rep. Prog. Phys. **64** (2001) 701; S. M. Reimann and M. Manninen: Rev. Mod. Phys. **74** (2002) 1283.
- 2) D. Goldhaber-Gordon, H. Shtrikman, D. Mahalu, D. Abusch-Magder, U. Meirav, and M. A. Kanster: Nature (London) **391** (1998) 156; D. Goldhaber-Gordon, J. Göres, M. A. Kastner, H. Shtrikman, D. Mahalu, and U. Meirav: Phys. Rev. Lett. **81** (1998) 5225.
- 3) S. M. Cronenwett, T. H. Oosterkamp, and L. P. Kouwenhoven: Science **281** (1998) 540.
- 4) T. K. Ng and P. A. Lee: Phys. Rev. Lett. **61** (1988) 1768.
- 5) L. I. Glazman and M. E. Raikh: JETP Lett. **47** (1988) 452.
- 6) A. Kawabata: J. Phys. Soc. Jpn. **60** (1991) 3222.
- 7) Y. Meir and N. S. Wingreen: Phys. Rev. Lett. **68** (1992) 2512; Y. Meir, N. S. Wingreen, and P. A. Lee: Phys. Rev. Lett. **70** (1993) 2601; A. -P. Jauho, N. S. Wingreen, and Y. Meir: Phys. Rev. B **50** (1994) 5528.
- 8) A. Oguri, H. Ishii, and T. Saso: Phys. Rev. B **51** (1995) 4715.
- 9) For review, see *Proceedings of the NATO Advanced Research Workshop on Mesoscopic Superconductivity*, edited by F. W. J. Hekking, G. Schön, and D. V. Averin: Physica B **203** (1994); C. J. Lambert and R. Raimondi: J. Phys.: Condens. Matter **10** (1998) 901.
- 10) C. W. J. Beenakker: Phys. Rev. B **46** (1992) 12841.
- 11) H. -K. Zhao and G. v. Gehlen: Phys. Rev. B **58** (1998) 13660.
- 12) Q. -f. Sun, J. Wang, and T. -h. Lin: Phys. Rev. B **59** (1999) 3831; Phys. Rev. B **59** (1999) 13126; Phys. Rev. B **62** (2000) 648.
- 13) P. Recher, E. V. Sukhorukov, and D. Loss: Phys. Rev. B **63** (2001) 165314.
- 14) H. -K. Zhao and J. Wang: Phys. Rev. B **64** (2001) 094505.
- 15) Z. Chen, J. Wang, B. Wang, and D. Y. Xing: Phys. Lett. A **334** (2005) 436.
- 16) R. Fazio and R. Raimondi: Phys. Rev. Lett. **80** (1998) 2913; **82** (1999) 4950(E).
- 17) P. Schwab and R. Raimondi: Phys. Rev. B **59** (1999) 1637.
- 18) S. Y. Cho, K. Kang, and C. -M. Ryu: Phys. Rev. B **60** (1999) 16874.
- 19) A. A. Clerk, V. Ambegaokar, and S. Hershfield: Phys. Rev. B **61** (2000) 3555.
- 20) Q. -f. Sun, H. Guo, and T. -h. Lin: Phys. Rev. Lett. **87** (2001) 176601.
- 21) J. C. Cuevas, A. L. Yeyati, and A. Martín-Rodero: Phys. Rev. B **63** (2001) 094515.
- 22) Y. Avishai, A. Golub, and A. D. Zaikin: Phys. Rev. B **63** (2001) 134515; Europhys. Lett. **55** (2001) 397.
- 23) T. Aono, A. Golub, and Y. Avishai: Phys. Rev. B **68** (2003) 045312.
- 24) A. Golub and Y. Avishai: Phys. Rev. B **69** (2004) 165325.
- 25) M. Krawiec and K. I. Wysokiński: Supercond. Sci. Technol. **17** (2004) 103.
- 26) J. Splettstoesser, M. Governale, J. König, F. Taddei, and R. Fazio: cond-mat/0612257.
- 27) T. Domański, A. Donabidowicz, and K.I. Wysokiński: cond-mat/0612440.
- 28) M. R. Gräber, T. Nussbaumer, W. Belzig, and C. Scönnenberger: Nanotechnology **15** (2004) S479; M. R. Gräber, T. Nussbaumer, W. Belzig, T. Kontos, and C. Scönnenberger: cond-mat/0406638.
- 29) H. R. Krishna-murthy, J. W. Wilkins, and K. G. Wilson: Phys. Rev. B **21** (1980) 1003; (1980) 1044.
- 30) A. C. Hewson: *The Kondo Problem to Heavy Fermions* (Cam-

- bridge University Press, Cambridge, 1993).
- 31) M. -S. Choi, M. Lee, K. Kang, and W. Belzig: Phys. Rev. B **70** (2004) 020502.
- 32) A. Oguri, Yoshihide Tanaka, and A. C. Hewson: J. Phys. Soc. Jpn. **73** (2004) 2494.
- 33) Yoshihide Tanaka, A. Oguri, and A. C. Hewson: cond-mat/0606581.
- 34) I. Affleck, J. -S. Caux, and A. M. Zagoskin: Phys. Rev. B **62** (2000) 1433.
- 35) O. Sakai, Y. Shimizu, and T. Kasuya: Prog. Theor. Phys. Suppl. **108** (1992) 73.
- 36) K. Satori, H. Shiba, O. Sakai, and Y. Shimizu: J. Phys. Soc. Jpn. **61** (1992) 3239.
- 37) A. C. Hewson, A. Oguri, and D. Meyer: Eur. Phys. J. B **40** (2004) 177.
- 38) T. Soda, T. Matsuura, and Y. Nagaoka: Prog. Theor. Phys. **38** (1967) 551.
- 39) H. Shiba and T. Soda: Prog. Theor. Phys. **41** (1969) 25.
- 40) E. Müller-Hartmann and J. Zittartz: Z. Phys. **234** (1970) 58.
- 41) T. Matsuura: Prog. Theor. Phys. **57** (1977) 1823.